Silver nanoparticle–*E. coli* colloidal interaction in water and effect on *E. coli* survival

A. Dror-Ehre [a],[*], H. Mamane [b], T. Belenkova [c], G. Markovich [c], A. Adin [a]

[a] Department of Soil and Water Sciences, Faculty of Agriculture, Food and Environment, The Hebrew University of Jerusalem, Rehovot 76100, Israel
[b] School of Mechanical Engineering, Tel Aviv University, Tel Aviv 69978, Israel
[c] School of Chemistry, Tel Aviv University, Tel Aviv 69978, Israel

A R T I C L E   I N F O

A B S T R A C T

Silver nanoparticles exhibit antibacterial properties via bacterial inactivation and growth inhibition. The mechanism is not yet completely understood. This work was aimed at elucidating the effect of silver nanoparticles on inactivation of *Escherichia coli*, by studying particle–particle interactions in aqueous suspensions. Stable, molecularly capped, positively or negatively charged silver nanoparticles were mixed at 1 to 60 $\mu g \, mL^{-1}$ with suspended *E. coli* cells to examine their effect on inactivation of the bacteria. Gold nanoparticles with the same surfactant were used as a control, being of similar size but made up of a presumably inert metal. Log reduction of $5 \log_{10}$ and complete inactivation were obtained with the silver nanoparticles while the gold nanoparticles did not show any inactivation ability. The effect of molecularly capped nanoparticles on *E. coli* survival was dependent on particle number. Log reduction of *E. coli* was associated with the ratio between the number of nanoparticles and the initial bacterial cell count. Electrostatic attraction or repulsion mechanisms in silver nanoparticle–*E. coli* cell interactions did not contribute to the inactivation process.

© 2009 Elsevier Inc. All rights reserved.

1. Introduction

Silver in its ionic form (Ag^+) is an environmentally friendly antimicrobial that is commonly used against many species of bacteria, including *Escherichia coli* [1–5]. Recent investigations of silver in the form of nanoparticles (Ag-NPs) have demonstrated a similar effect at lower concentrations than with the ionic form: effective concentrations of Ag-NPs and Ag^+ have been reported in the nanomolar and micromolar ranges, respectively [6,7]. NPs generally exhibit inherent unique characteristics, such as large specific surface area, modified structure, controlled surface composition and reactivity, which endow them with remarkable physical, chemical and biological properties [6–9]. The development of new preparation methods that yield high concentrations and stable dispersions of Ag-NPs has led to a broader range of antibacterial applications [10–14].

Although Ag-NPs have been shown to effectively inactivate bacteria and inhibit microbial growth [8,11,15–21], the mechanism has yet to be fully elucidated. The bactericidal property of Ag-NPs is partially similar to that of silver ions [7]. Ag-NPs, like silver ions, attach to phosphate and sulfur groups that are part of the phospholipid cell membrane or to membranal proteins [8,22] and severely damage the cell and its major functions, such as permeability, regulation of enzymatic signaling activity, and cellular

oxidation and respiratory processes [7,16,18,23]. Ag-NPs can penetrate the bacterial cell and accumulate to toxic levels that may cause death of the organism [22]. In addition, Ag-NPs can bind to the DNA inside the bacterial cells, preventing its replication [1,8], or interact with the bacterial ribosome [24]. Both Ag^+ and free radicals derived from the Ag-NPs have been suggested to be responsible for the antimicrobial activity [8,12,17].

Recent studies have focused on some of the physicochemical properties of Ag-NPs, to identify exactly which of these particles' physical or chemical properties is responsible for the effect on microorganisms. Ag-NPs' inactivation of *E. coli* has been found to be associated with NP concentration [7,18], bacterial type [17,18], NP shape [17], the presence of Ag(I) [18] and NP size [8,10,15,18]. Moreover, bacterial growth in the presence of a given concentration of silver has been found to be dependent on the initial number of cells [7,18]. In the present study, an integrated approach was used to elucidate the combined impact of Ag-NP particle size, dose and initial number of bacterial cells on inactivation of planktonic cells suspended in water. To date, most of the applications involving Ag-NP bactericidal activity have dealt with interaction of bacteria with silver Ag-NP immobilized on agar plates [7,8,17]. However, this study examined a pretreatment technique based on the application of Ag-NPs in suspension. Such a pretreatment can be effective in controlling the formation of biofouling in water systems, such as distribution pipelines or membrane-filtration processes. The bactericidal activity of the NPs is hypothesized to be associated with the ratio between the number of NPs and the

---

[*] Corresponding author. Fax: +972 8 9475181.
E-mail address: adin@vms.huji.ac.il (A. Dror-Ehre).

number of bacterial cells. Thus, a higher ratio will increase the frequency of particle-bacterium collisions and attachment and increase bacterial inactivation.

Previous studies have suggested electrostatic repulsion or attraction as the mechanism underlying the bactericidal properties of Ag-NPs [24,25]. The bacterial surface is negatively charged due carboxylic and phosphonate groups in the outer membrane [24]. However, both Ag-NPs with negative zeta potential and charge [8,17,18] and metal oxide NPs with positive zeta potential and charge [24], as well as positively charged silver ions [26], have shown bactericidal activity. Although electrostatic forces between particles are expected, electrostatic attraction as a significant mechanism for NP attachment to bacteria has never been studied.

In the present study, negatively or positively charged molecularly capped Ag-NPs (Ag-MCNPs) were prepared to elucidate the influence of capping agent charge on the NPs' ability to inactivate planktonic E. coli suspended in water, to inhibit bacterial growth and to further support the hypothesized numerical particulate ratio approach. The experiments were carried out in aqueous suspensions containing varying amounts of NPs and E. coli cells.

2. Materials and methods

2.1. Materials

E. coli ATCC 35218 was purchased from Hy-Labs (Rehovot, Israel). The Luria–Bertani (LB) medium used to grow and maintain the bacterial culture was supplied by Difco Laboratories, and consisted of (in 1 L): 10 g tryptone, 5 g yeast extract and 5 g NaCl. 3-Mercaptopropionic acid (MPA; 99%) was obtained from Aldrich. Silver nitrate was obtained from Carlo Erba reagents. Sodium borohydride (NaBH$_4$; 99%) and polylysine (PL) 26,300 MW were obtained from Sigma–Aldrich, as was hydrogen tetrachloroaurate(III) trihydrate.

2.2. Preparation of Ag-MCNPs and Au-MCNPs

NP synthesis is based on reducing metal ions in solution in the presence of several types of stabilizing agents. As the source of silver ions, 50 mL of 0.04 M aqueous silver nitrate (AgNO$_3$) was mixed with 0.33 mL of 0.3 M MPA as an anionic stabilizing agent or 16.7 mL of 4.8 mM PL as a cationic stabilizing agent. The solution was stirred and the pH adjusted to 7 using NaOH. Fifty milliliter of 0.004 M NaBH$_4$ was added slowly to the solution in order to reduce the Ag ions. A dark brown color appeared while adding the NaBH$_4$ until the solution appearance stabilized. Finally, stable MCNPs with negative or positive charge were obtained. A dispersion of particles with a relatively narrow size distribution was obtained after removing the larger particles and aggregates by centrifugation at 20,000 rcf for 10 min for Ag-PL particles and centrifugation at 20,000 rcf for 30 min for Ag-MPA particles. Gold NPs (Au-MCNPs) were synthesized following the same protocol with 50 mL of 0.004 M aqueous gold chloride trihydrate used as the source of the gold ions.

2.3. Methodology for studying the effect of MCNPs on E. coli inactivation

E. coli ATCC 35218 was grown in 80 mL liquid LB medium to mid-log phase (OD$_{570}$ of about 0.4). E. coli in the range of 10^5–10^8 colony forming units (CFU) was suspended in 1 mL distilled water supplemented with negatively or positively surface-charged MCNPs. The particle concentration in the suspensions varied from 1 to 60 μg mL^{-1}. Those μg/ml concentrations were directly calculated from the final molar concentration of the silver inserted in

the preparation. A similar suspension without NPs was used as a control. A suspension of Au-MCNPs with the same surfactants and average size was used as another similarly sized but presumably inert metal control for the NPs. Pure surfactant solutions (PL, MPA) were used as vehicle controls. The suspensions of bacteria and NPs were thoroughly vortexed for 1 min and 50-μL aliquots were cultured on LB agar plates. The plates were incubated at 37 °C for 24 h. Colonies were counted and log reduction (log$_{10}N_0$/N) for each treatment was calculated relative to the colony count of untreated bacteria (N_0), with N representing the number of bacteria (CFU) that survived the treatment. All experiments were performed in triplicate under sterile conditions.

The interaction between E. coli and NPs was examined by transmission electron microscopy (TEM). For specimen preparation, samples containing distilled water, 10^7 CFU mL^{-1} E. coli and 45 μg mL^{-1} Ag-MCNPs or Au-MCNPs were prepared. A 10-μL drop was deposited on a TEM copper grid with a lacy carbon film. To fix the bacteria, the grids were exposed to 2.5% (v/v) glutaraldehyde in PBS solution for 30 min. Grids were washed three times in PBS and three times in distilled water, to remove salt and buffer deposits. The bacteria-NP specimens were imaged in a FEI Tecnai F20 TEM.

2.4. Methodology for studying the effect of Ag-MCNPs on bacterial growth rate

A fresh colony of mid-log phase E. coli (10^8 CFU mL^{-1}) grown in LB medium was thoroughly mixed with 50 μg mL^{-1} Ag-PL (sample PL50) and 33 μg mL^{-1} Ag-PL (sample PL33) in water. Aliquots (2 mL) of each suspension (treated or non-treated bacteria) were inoculated into 100 mL fresh LB medium (without NPs). The suspensions were agitated in a shaker bath. Growth trends were monitored by OD$_{570}$ measurements performed at predetermined intervals. The spectrophotometry reference was the same LB medium without bacteria.

2.5. Characterization

The OD of the bacterial cultures in liquid LB medium was evaluated using a UV200RS spectrophotometer. Particle size distribution, average particle size, morphology and colloidal stability of the Ag-MCNPs were characterized by TEM. The size characterization of the samples was carried out on TEM images using the Digital Micrograph software by Gatan. The data were statistically analyzed using OriginPro 6.1 software. Zeta potential measurements were made in an electrophoretic light-scattering apparatus (Zeta Sizer-Nano series Malvern Instruments) to examine NP colloidal stability and charge.

3. Results and discussion

Under the conditions used to prepare the Ag-MCNPs, the particles had a roughly spherical shape with a relatively narrow size distribution, formed stable dispersions, and were positively or negatively charged. Zeta potential values were 40.2 mV and −46.1 mV for the positive Ag-PL and negative Ag-MPA particles, respectively. These values are characteristic of stable colloids [27]. The anionic capping agent, MPA, is a small, widely available, inexpensive anionic surfactant from the family of thiol-containing molecules. Thiol groups form strong bonds to gold and silver surfaces making them the optimal anchor group and the carboxyl group provides the negative charge at neutral pH. Analogous amine-containing thiols that should be able to provide the positively charged counterpart at neutral pH are not able to stabilize the Ag-NP colloidal dispersion. A possible reason for this asymmetry is the high affinity of the amine group to the silver and gold surfaces. The bifunctional
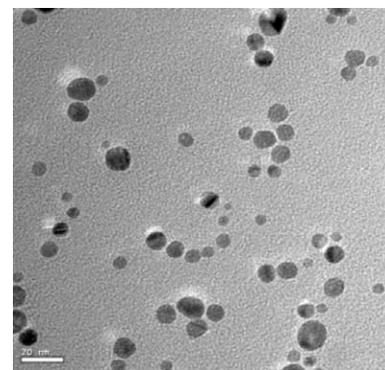
Table 1
Characteristics of Ag-MCNPs.

Type	Surfactant and charge	Centrifugation condition (rpm/min)	Mean size (nm)	Standard deviation (nm)
A	PL – Positive	13,500/10	7.2	2.8
B	MPA – Negative	13,500/30	6.7	2.9
C	PL – Positive	–	12.5	3.5
D	MPA – Negative	–	15	5

thiol-amine molecules act as efficient crosslinkers between the NPs, inducing their aggregation and precipitation. Thus, for cationic Ag-NPs, low-molecular-weight PL was found to be an excellent surfactant, generating stable dispersions of isolated single or a few particles with a high zeta potential value, indicating high positive charge density at the PL-coated particle surfaces with minimal interparticle crosslinking, probably due to the strong electrostatic and steric repulsions.

Table 1 displays the details of the various NP samples (A–D), indicating surfactant type and charge, centrifugation conditions and the resulting mean size. Two substantially different mean sizes for each of the MPA- and PL-coated MCNPs were obtained. Fig. 1 shows size-distribution histograms of particle types A and B which were evaluated by analyzing the TEM micrographs. Fig. 2 presents a representative TEM micrograph of type A NPs which appear well-dispersed upon stabilization with PL.

The effect of MCNPs on the viability of planktonic E. coli cells suspended in water was assumed to be associated with the interaction between the Ag-NPs and the suspended microorganism (also termed biocolloid). The experimental setup therefore included varying amounts of the two types of particles (i.e. NPs and biocolloids). The MCNPs were stable when diluted in water with the E. coli as no precipitation was observed.

The role of MCNP charge in determining the interactions between NPs and bacteria is not yet completely understood. Some studies have postulated that the electrostatic attraction between negatively charged membrane components and the positively charged NP surface is crucial for the interaction between bacteria and NPs [8,17]. In contrast, Stoimenov et al. [25] and Hamouda and Baker [28] assumed that particles with the same charge as the bacteria induce electrostatic repulsion and prevent the interaction between the particles. Fig. 3 presents the impact of MCNP surface charge and concentration on log inactivation of planktonic E. coli in water. An increase in the concentration of NPs with either positive or negative charge resulted in a similar increase in log inactivation. An increase in the bactericidal activity of Ag-NPs in the solid state has also been shown with increasing NP concentra-


Fig. 2. TEM micrograph of stable type A NPs (bar = 20 nm).
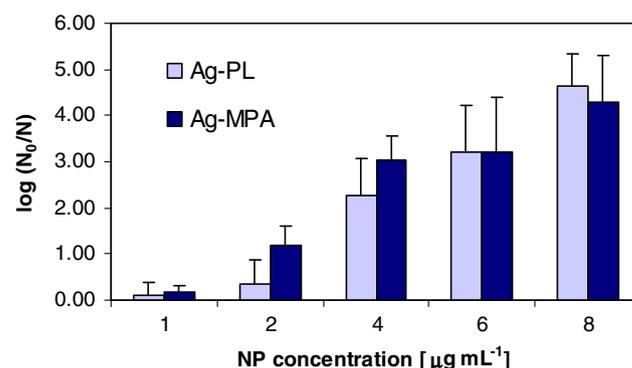
Fig. 3. Impact of surface charge and various concentrations of MCNPs on bacterial inactivation. $N_0 = 2.4 \times 10^7$ CFU mL^{-1}.

tion [8,11,15–18]. One of the main focuses of such studies has been the development of antibacterial surfaces with biocidal activity for a variety of applications. However, the aqueous suspension of NPs in the present study can be used as a disinfectant in water systems prior to membrane-filtration processes. Complete inhibition of E. coli was observed at much lower silver concentrations than those needed to obtain a similar effect with surface-supported particles [11]. Thus, mixing the MCNPs with the biocolloids afforded enhanced inactivation, probably due to the higher probability of collision between the NPs and biocolloids in suspension. Moreover, Ag-PL and Ag-MPA at 8 μg mL^{-1} showed an approximately 5 log$_{10}$ reduction with similar standard deviations. These results imply that under the experimental conditions, the influence of
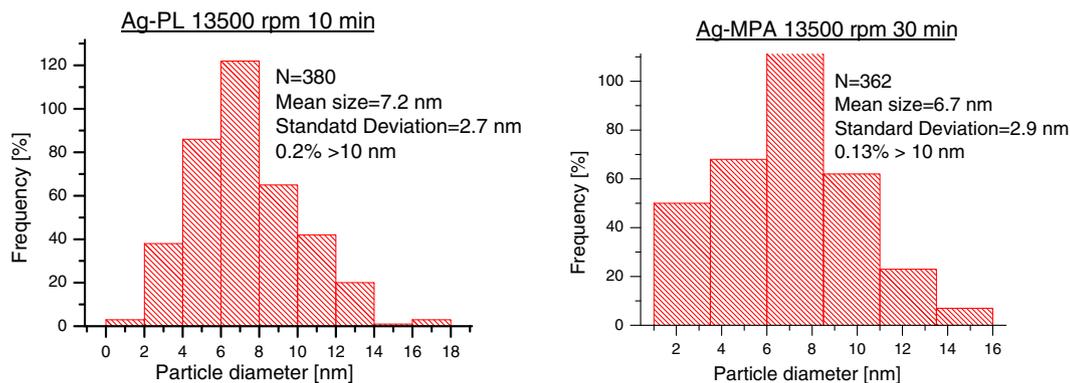
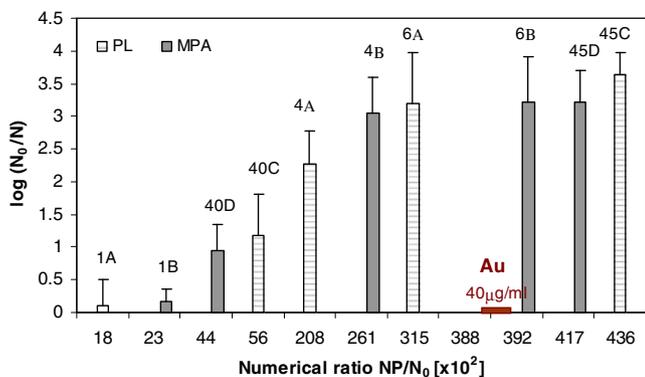**Fig. 1.** Particle-size distribution histogram of MCNPs.

Fig. 4. Bacterial inactivation versus NP/N_0. The number and letter above each column represent concentration in µg mL^{-1} and type of MCNP, respectively.

Fig. 5. Inactivation presented as log ($N + 1$) versus the NP/N_0 ratio.

electrostatic attraction or repulsion between the MCNPs and the negatively charged components in the *E. coli* membrane is probably insignificant for bacterial inactivation.

The effect of Ag-NP size on bacterial activity has been demonstrated previously, indicating that small particles are more active than larger particles per identical unit of silver mass [6,8,10,16]. The mean diameter of each NP type (PL or MPA Ag-NPs as presented in Table 1), its concentration and silver density were used to estimate the number density of the particles. The ratio between the number of NPs and the number of biocolloids (NP/N_0) was calculated for each sample. Fig. 4 illustrates the inactivation ability of MCNP types A–D in relation to the NP-to-biocolloid ratio. Type B MCNPs at 6 µg mL^{-1} and type D MCNPs at 45 µg mL^{-1} showed similar NP/N_0 ratios and similar log$_{10}$ reductions. The activity of Au-MCNPs is also presented in Fig. 4 and, as expected, the treatment with gold NPs did not result in inactivation beyond an estimated threshold of 0.5 a log. Pure surfactant solutions, which were used as vehicle controls, showed nearly 100% survival of *E. coli*. These results are consistent with findings by Li et al. [21] who reported an improved antimicrobial effect with increasing NP concentration. While other researchers have observed the dependence on particle size, the present work clearly demonstrates that within a size range of approximately 5–15 nm, the important parameter is the NP/N_0 ratio rather than NP size itself. Fig. 4 supports this assumption by show general trend of inactivation increase with increase in NP/N_0 ration.

The effect of the initial number of bacterial cells on the extent of inactivation by Ag-NPs has been previously reported [7,18]. To elucidate this phenomenon within the framework of a particle-cell interaction approach, for a fixed MCNP concentration, the concentration of the bacteria was varied. Fig. 5 presents the logarithmic number of cells surviving treatment versus the NP-to-biocolloid ratio. The experiment was conducted with mid-log phase bacteria diluted by a factor of 10 to obtain 10^5–10^8 CFU mL^{-1} of biocolloids, which were mixed with type A MCNPs at a concentration of 2, 7 or 12 µg mL^{-1}. The logarithmic number of cells surviving the treatment is expressed as log ($N + 1$) following the approach used by Pal et al. [7], which allows a logarithmic presentation of samples in which no colonies are detected in a treated volume (50 µL and complete inactivation $N = 0$). Initially, for low NP-to-biocolloid ratios, a constant high level of survival was observed up to about 1000 NPs per bacterium. Above this a first-order linear relationship was observed between the log of surviving bacterial cells and the NP-to-biocolloid ratio. Complete inactivation was observed at a ratio of approx. 2×10^6. Regression analysis was performed on all the data fields used to fit the linear sections of the log inactivation curve with regression coefficient (R^2) of 0.98. The linear curve was described by the following equation:
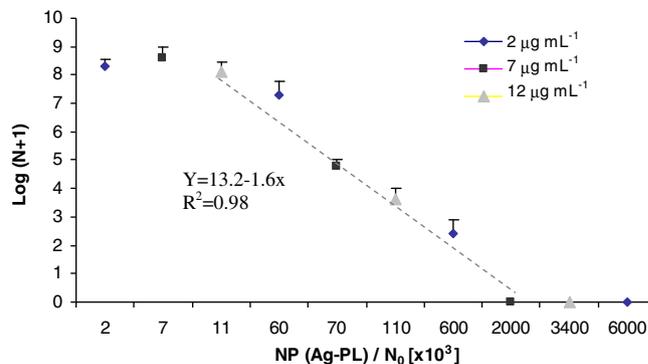
$$\log(N + 1) = A - BNP/N_0 \qquad (1)$$

where A and B are empirical coefficients. Under these conditions, A and B were found to be 13.2 and 1.6, respectively. This equation can be used to evaluate the inactivation potential of NPs at given concentrations of Ag-NPs and bacteria.

In Fig. 4, the concentration of bacteria was fixed while the concentrations of MCNPs varied, while in Fig. 5 for each MCNP (Ag-PL) concentration (2, 7, 12 µg mL^{-1}), the concentration of bacteria was varied. Thus, in both cases, the log inactivation of planktonic *E. coli* depends on the NP/N_0 ratio.

It is suggested that the inactivation effect of MCNPs on bacteria is associated with collision and attachment efficiencies (so-called successful collision) between two particles of different sizes-NPs which are in the nanometer size range and biocolloids (bacteria cells) which are in the micrometer size range. While the collision frequency relies mainly on particle-transport mechanisms, such as hydraulic shear or diffusion, it can be expected that the attachment probability will be a function of the physicochemical properties of the MCNPs, such as charge, size or interface structure. Here we found that the impact of MCNPs on the tested bacteria is independent of charge. Further study is needed to examine interface structure as a crucial factor. The suspensions in this work were sheared by mixing, implying that the dominant transport factor was a velocity gradient rather than Brownian motion. In this case, the frequency of collisions, according to the classical Smoluchowski approach [29], is a function of the sum of the two particles' diameters to the third power, the velocity gradient and the particles' concentration (number of NPs and biocolloids) as presented in:

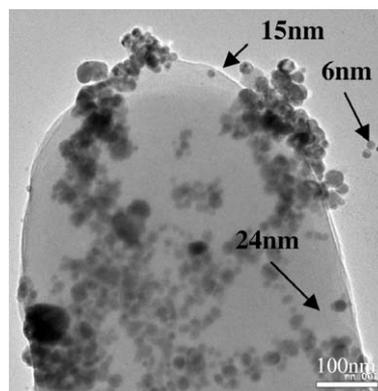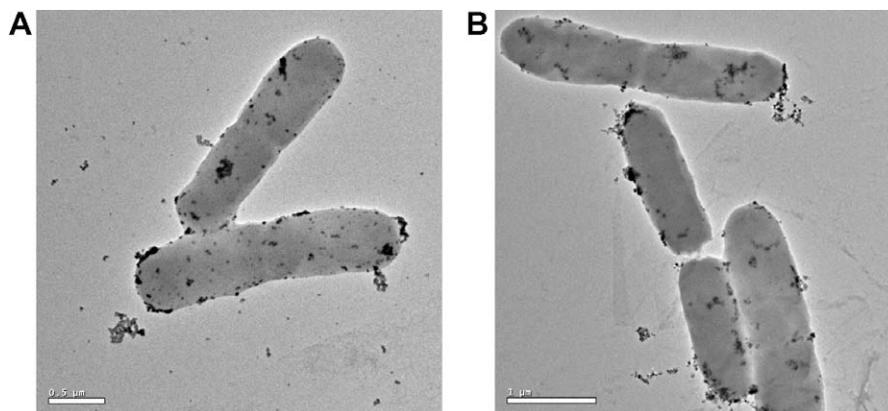$$J_{ij} = \frac{1}{6} N_i N_j G (d_i + d_j)^3 \qquad (2)$$

Fig. 6. TEM micrograph of *E. coli* after treatment with Ag-MCNPs. Bar = 100 nm.

Fig. 7. TEM micrograph of *E. coli* treated with MCNPs. (A) Au-MCNPs (bar = 0.5 μm). (B) Ag-MCNPs (bar = 1 μm).

where J is the frequency of collisions per unit volume between particle types i and j, N_i and N_j are their number densities, and d_i and d_j are the respective diameters.

Generally, the diameters of the MCNPs and the bacteria differ by two orders of magnitude. Hence, the impact of NP size on collision rate is negligible. The mixing time, i.e. 10 min of shaking followed by a few seconds of vortexing, was kept constant in all samples.

This particulate approach assumes that the inactivation effect increases with increasing number of NPs that can be attached to a bacterium. The results presented in Figs. 4 and 5 support this assumption and also explain the previously reported dose and size dependencies.

Previous reports have found Ag-NPs attached to bacterial cell membranes as well as NPs inside the cells. Morones et al. [8] indicated that only NPs with a diameter of less than 10 nm exhibit a direct interaction with a few bacterial strains, including *E. coli* and *Pseudomonas aeruginosa*. Xu et al. [30], on the other hand, showed that Ag-NPs with sizes of up to 80 nm accumulate inside living *P. aeruginosa* cells, demonstrating that these Ag-NPs had been transported through the cells' outer and inner membranes [30]. Figs. 6 and 7 show TEM micrographs of Ag-MCNPs and Au-MCNPs attached to *E. coli*. Although visually, both micrographs appear similar, the particles' inactivation properties are different: as opposed to Ag-MCNPs, Au-MCNPs did not show any inactivation ability. *E. coli*, a gram-negative bacterium, has a layer of peptidoglycan and a layer of lipopolysaccharide, both of which lack strength and rigidity [30]. This structure gives the NPs accessibility to anchoring sites on the cell wall [16]. It is assumed that the inactivation ability of MCNPs is associated with the number of successful NP attachments to anchoring sites.

Growth inhibition of bacteria grown in a liquid medium supplemented with Ag-NPs has been previously shown [7,16,18]. In the present study, the bacteria were treated with Ag-PL before addition into a LB medium without NPs. In Fig. 8, bacterial growth curves are shown for the non-treated control bacteria and bacteria pretreated with 33 and 50 μg mL^{-1} Ag-PL. Aliquots of 2 mL were added into 200 mL LB medium for the control and PL33, and into 100 mL LB medium for PL50. A 5.6 log$_{10}$ reduction in bacterial count was found in the aliquot pre-treated with PL50. The first observation in Fig. 8 is that the kinetics of the growth process in all three curves follows typical bacterial population growth curves (a lag phase in which the bacteria are adapting to fresh medium, an exponential growth phase and a stationary phase with no net population increase or decrease) [31]. Under the experimental conditions, the lag phase of the treated bacteria was found to be more prolonged than that of the untreated bacteria, and the final population in the stationary phase was similar for the two treatment types but higher for the control. These results suggest that Ag-NPs can inhibit bacterial growth. Further studies are needed to explore the dependence of growth rate on the MCNP/N_0 ratio.
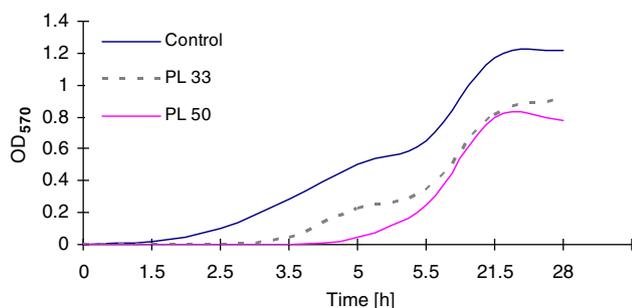
4. Conclusions

The inactivation effect of Ag-MCNPs on *E. coli* can be described by a colloid-particle interaction model. This effect was dependent on particle number, and log inactivation of *E. coli* showed a linear fit with the ratio between the number of NPs and the number of biocolloid particles measured as the initial bacterial cell count. This can be explained by an increase in NP-bacterium collision frequency. Au-MCNPs did not show any inactivation ability. Electrostatic attraction or repulsion between the Ag-MCNP and *E. coli* cell did not contribute to the inactivation process.

Fig. 8. Growth curves for Ag-PL treated and control *E. coli* in LB medium, measured by solution OD.

References

[1] Q.L. Feng, J. Wu, G.O. Chen, F.Z. Cui, T.N. Kim, J.O. Kim, J. Biomed. Mater. Res. 52 (2000) 662.
[2] N. Silvestry-Rodriguez, E.E. Sicairos-Ruelas, C.P. Gerba, K.R. Bright, Rev. Environ. Contam. Toxicol. 191 (2007) 23.
[3] H. Gentry, S. Cope, Nurs. Stand. 19 (2005) 51.
[4] V.K. Poon, A. Burd, Burns 30 (2004) 140.
[5] G. Zhao, S.E. Stevens, BioMetals 11 (1998) 27.
[6] C.N. Lok, C.M. Ho, R. Chen, Q.Y. He, W.Y. Yu, H. Sun, P.K.H. Tam, J.F. Chiu, C.M. Che, J. Proteome Res. 5 (2006) 916.
[7] S. Pal, Y.K. Tak, J.M. Song, Appl. Environ. Microbiol. 73 (2007) 1712.

[8] J.R. Morones, J.L. Elechiguerra, A. Camacho, K. Holt, J. Kouri, J.T. Ramirez, M.J. Yacaman, Nanotechnology 16 (2005) 2346.
[9] U.K. Parashar, P.S. Saxena, A. Srivastava, Digest. J. Nanomater. Biostruct. 3 (2008) 81.
[10] A. Panacek, R. Prucek, M. Kolar, R. Vecerova, L. Kvitek, R.N. Pizurova, V.K. Tatjana, R. Zboril, J. Phys. Chem. B 110 (2005) 16248.
[11] I. Sondi, D.V. Goia, E. Matijevic, J. Colloid Interface Sci. 260 (2003) 75.
[12] E.J. Fernandez, J. Garcia-Barrasa, A. Laguna, J.M. Lopez-de-Luzuriaga, M. Monge, C. Torres, Nanotechnology 19 (2008) 1.
[13] M.Z. Kassaee, A. Akhavan, N. Sheikh, R. Beteshobabrud, Radiat. Phys. Chem. 77 (2008) 1074.
[14] R.C. Doty, T.R. Tshikhudo, M. Brust, D.G. Fernig, Chem. Mater. 5 (2005) 4630.
[15] C. Baker, A. Pradhan, L. Pakstis, D.J. Pochan, S.J. Shah, J. Nanosci. Technol. 5 (2005) 244.
[16] S. Shrivastava, T. Bera, A. Roy, G. Singh, P. Ramachandrarao, D. Dash, Nanotechnology 18 (2007) 1.
[17] J.S. Kim, E. Kuk, K.N. Yu, J.H. Kim, S.H. Park, H.J. Lee, S.H. Kim, Nanomed.: Nanotechnol. Biol. Med. 3 (2007) 95.
[18] I. Sondi, B. Salopek-Sondi, J. Colloid Interface Sci. 275 (2004) 177.
[19] C.N. Lok, C.M. Ho, R. Chen, Q.Y. He, W.Y. Yu, H. Sun, P.K.H. Tam, J.F. Chin, C.M. Che, J. Biol. Inorg. Chem. 12 (2007) 527.
[20] K.Y. Yoon, J.H. Byeon, J.H. Park, J. Hwang. Sci. Tot. Environ. 373 (2007) 572.
[21] P. Li, J. Li, C.Z. Wu, Q.S. Wu, J. Li, Nanotechnology 16 (2005) 1912.
[22] D.W. Hatchett, H.S. White, J. Phys. Chem. 100 (1996) 9854.
[23] K.B. Holt, A.L. Bard, Biochemistry 44 (2005) 13214.
[24] M. Yamanaka, K. Hara, J. Kudo, Appl. Environ. Microbiol. 71 (2005) 7589.
[25] P.K. Stoimenov, R.L. Klinger, G.L. Marchin, K.J. Klabunde, Langmuir 18 (2002) 6679.
[26] P. Dibrov, J. Dzioba, K.K. Gosink, C.C. Hase, Antimicrob. Agents Chemother. 46 (2002) 2668.
[27] D.F. Evans, H. Wennerstrom, The Colloidal Domain, Wiley, New York, 1999, p. 428.
[28] T. Hamouda, J. Baker, J. Appl. Microbiol. 89 (2000) 397.
[29] J. Gregory, Particles in Water: Properties and Processes, Taylor & Francis, Boca Raton, FL, 2006, p. 93.
[30] X.H.N. Xu, W.J. Brownlow, S.V. Kyriacou, Q. Wan, J.J. Viola, Biochemistry 43 (2004) 10400.
[31] T.D. Brock, M.T. Madigan, Biology and Microorganisms, Prentice Hall, New Jersey, 1991, p. 312.